Singlet Fission in Poly(9,9'-di-*n*-octylfluorene) Films

Yasunari Tamai,[†] *Hideo Ohkita,*[*,†,‡] *Hiroaki Benten,*[†] *and Shinzaburo Ito*[†]

[†]Department of Polymer Chemistry, Graduate School of Engineering, Kyoto University, Katsura, Nishikyo, Kyoto 615-8510, Japan, and [‡]Japan Science and Technology Agency (JST), PRESTO, 4-1-8 Honcho Kawaguchi, Saitama 332-0012, Japan

E-mail: ohkita@photo.polym.kyoto-u.ac.jp

RECEIVED DATE (to be automatically inserted after your manuscript is accepted if required according to the journal that you are submitting your paper to)

CORRESPONDING AUTHOR FOOTNOTE.

[†]Kyoto University.

[‡]JST PRESTO.

TITLE RUNNING HEAD: Singlet Fission in Polyfluorene Films

Abstract

The dynamics of singlet fission in poly(9,9'-di-*n*-octylfluorene) (PFO) films was studied by transient absorption spectroscopy. Under a high excitation intensity, triplet excitons were rapidly interconverted from singlet excitons on a picosecond time stage. From the excitation intensity dependence of the generation yield, the rapid triplet exciton formation is attributed to the singlet fission from a higher singlet excited state S_n formed by the singlet–singlet annihilation (singlet fusion followed by singlet fission). The singlet fission from the S_n state was about two times more efficient in amorphous PFO films than in ordered *β*-PFO films, in which the conjugated main chains are planarly extended and aligned. On the other hand, about a half of triplet pairs were deactivated in the amorphous PFO film through the triplet–triplet annihilation with a time constant of 1.7 ns, while no triplet pair decay was observed in the *β*-PFO film. As a result, the overall triplet generation yield was comparable in these films. The decrease in the fission efficiency in the *β*-PFO is discussed in terms of the presence of another relaxation pathway from the S_n state. The efficiency of triplet pair dissociation is discussed in terms of the triplet exciton diffusion.

KEYWORDS (Word Style "BG_Keywords"). polyfluorene, singlet fission, annihilation, *β* phase, transient absorption, charge dissociation

BRIEFS (WORD Style "BH_Briefs"). If you are submitting your paper to a journal that requires a brief, provide a one-sentence synopsis for inclusion in the Table of Contents.

1. Introduction

Singlet fission is an interconversion process in which one singlet excited state delocalized over neighboring two chromophore units is converted into two triplet excited states.[1–3] Because of the potential to improve the efficiency in organic photovoltaics (OPVs) by multiple exciton generation from one photon,[4–10] the singlet fission has attracted increasing attention recently. Since the first report of singlet fission in anthracene crystals,[11] a lot of experimental and theoretical studies have been published for various molecular crystals such as larger polyacenes (tetracene, pentacene).[2,3,12–19] In contrast, singlet fission in conjugated polymers has been reported only for limited materials,[2,3,20–27] and hence is not fully understood.

The efficiency of singlet fission is dependent on the sample morphology. In small molecular systems, singlet fission is generally more efficient in molecular crystals rather than in less ordered films. For example, the singlet fission efficiency in pentacene is nearly 100% for single crystals but is as low as 2% for vapor deposited polycrystalline films.[28,29] In contrast, different morphology dependences have been reported for conjugated polymers. For example, efficient singlet fission from a higher singlet excited state has been reported for amorphous films of regiorandom P3HT (RRa-P3HT) while no triplet exciton formation is observed for crystalline films of regioregular P3HT (RR-P3HT).[27] This is in sharp contrast with the singlet fission in small molecules. The absence of singlet fission in RR-P3HT crystalline films is attributed to preference polaron pair formation because of the large interchain interaction in π-stacked crystalline domains. On the other hand, both singlet fission and polaron pair formation have been reported for ladder-type poly(*p*-phenylene) (MeLPPP) films,[24,25,30] which exhibit highly ordered intrachain structures due to the planar main chain but do not form crystalline domains. Further studies are still needed to understand such characteristic morphology dependence of singlet fission in conjugated polymer films in more depth.

Herein, we study the singlet fission in poly(9,9'-di-*n*-octylfluorene) (PFO, chemical structure is shown in the inset of Figure 1) films by transient absorption spectroscopy. Focusing on the morphology dependence of the fission efficiency, we study the singlet fission in disordered amorphous PFO films

and in ordered PFO films with β phase. In the β phase, conjugated main chains are found to be planarly extended and aligned:[31–35] this is different morphology from crystalline phase in RR-P3HT or highly ordered intrachain structures in MeLPPP films. We perform spectroscopic analysis of triplet exciton formation and decay dynamics in amorphous and β-PFO films. As will be discussed later, singlet fission is observed in both amorphous and β-PFO films. The overall triplet generation yield is comparable in these films. Interestingly, however, the formation and decay dynamics of triplet excitons generated via singlet fission are significantly dependent on the film morphology. On the basis of transient absorption analyses, we discuss the origin of the difference in the triplet formation and decay dynamics in the two different PFO films.

2. Results

2.1. Absorption and Photoluminescence Spectra. As shown in Figure 1a, the PFO film prepared from chloroform exhibited a featureless absorption band at around 390 nm, which is characteristic of amorphous PFO films. In contrast, the PFO film prepared from chloroform with a 1,8-diiodooctane (DIO) additive showed a large absorption at around 400 nm and an additional sharp absorption at around 440 nm.[32] The sharp absorption at 440 nm is ascribed to the β-phase absorption in the film as reported previously.[35] Hereafter, this film is abbreviated as the β-PFO film. The β-phase absorption band is more pronounced with increasing concentration of the DIO additive. In this study, the β-phase volume fraction was fixed to about 35% to balance high β-phase fraction and film smoothness. Figure 1b shows the fluorescence spectra of amorphous and β-PFO films. The amorphous PFO film exhibited a fluorescence band at 420 nm, which is attributable to the fluorescence band of amorphous phase.[35] On the other hand, the β-PFO film showed a sharp 0–0 emission band at 440 nm with almost no Stokes shift, which is attributed to the β-phase emission.[35] Interestingly, no amorphous phase emission was observed at all for the β-PFO film even though the amorphous phase was selectively excited at 360 nm, suggesting rapid energy transfer from amorphous phase to β phase as reported previously.[36,37] Figure 1c shows the delayed photoluminescence spectra measured at 77 K by using a mechanical chopper. As

shown in the figure, two emission bands were observed at 420 and 600 nm for the amorphous PFO film and 440 and 600 nm for the *β*-PFO film. The emission bands at shorter wavelengths are the same as the fluorescence bands as shown in Figure 1b and thus ascribed to the delayed fluorescence probably because of triplet–triplet annihilation (TTA).[35] The emission bands at longer wavelengths are ascribed to the phosphorescence band of PFO films.[35] From the fluorescence and phosphorescence spectra, the energy levels of the lowest singlet and triplet excited states were estimated to be 2.93 and 2.11 eV for the amorphous PFO, and 2.81 and 2.09 eV for the *β*-PFO films, respectively.

-----<<< Figure 1 >>>-----

2.2. Transient Absorption Spectra.

Amorphous PFO: Figure 2a shows the transient absorption spectra of the amorphous PFO film measured from 0 ps to 3 ns after the laser excitation at 400 nm with high excitation intensity (~60 μJ cm^{-2}). Immediately after the laser excitation, a large absorption band was observed at 800 nm and two small absorption shoulders were observed at around 600 and 1000 nm. The transient spectrum at 0 ps is in good agreement with that observed under a low excitation intensity. Thus, all the absorption bands are ascribed to singlet excitons as reported previously.[35,38] These absorption bands decayed rapidly in the picosecond time domain. At 3 ns, the small absorption shoulders disappeared but an absorption band was observed at around 800 nm, suggesting that the band at 800 nm is different from singlet excitons. This absorption band was still observed at around 800 nm even in the microsecond time domain but decayed faster under an O_2 atmosphere. Therefore, the absorption band at 800 nm observed after nanoseconds is ascribed to triplet excitons in amorphous PFO films as reported previously.[34,38,39] No other long-lived transients were observed under this experimental condition.

β-PFO: Figure 2b shows the transient absorption spectra of the *β*-PFO film measured from 0 ps to 3 ns after the laser excitation at 400 nm with high excitation intensity (~60 μJ cm^{-2}). Immediately after the laser excitation, a large absorption band was observed at 800 nm, which is the same as that of the

amorphous PFO film, suggesting that singlet excitons are generated preferentially at amorphous phase in the *β*-PFO film by the 400-nm excitation. At 1 ps, this band was rapidly red-shifted to 850 nm with shoulders at 600 and 1000 nm, which is ascribed to singlet excitons in *β* phase, suggesting energy transfer from amorphous phase to *β* phase (details are described in the Supporting Information). Therefore, it can be safely said that singlet excitons in amorphous phase are negligible after a few picoseconds. At 3 ns, two sharp absorption bands were observed at around 650 and at 850 nm but no shoulder was observed, suggesting that the band at 850 nm is no longer assigned to singlet excitons in the *β* phase. These two bands were still observed even in the microsecond time domain. The band at 850 nm decayed faster under an O_2 atmosphere. Therefore, the long-lived absorption bands at around 650 and 850 nm are assigned to polaron and triplet excitons in *β*-PFO films, respectively, as reported previously.[39,40]

-----<<< Figure 2 >>>-----

2.3. Transient Absorption Decays.

Amorphous PFO: In order to observe the dynamics of singlet excitons selectively, we measured the transient absorption decay at 1050 nm. As shown in Figure 3, the transient signals of the singlet exciton decayed faster under higher excitation intensities. The decay curve was fitted with the sum of three exponential functions: $\Delta OD(t) = A_1 \exp(-t/\tau_1) + A_2 \exp(-t/\tau_2) + A_3 \exp(-t/\tau_3)$. The fitting parameters are summarized in Table 1. Here, the longest lifetime τ_3 was fixed to a fluorescence lifetime of 410 ps that was evaluated by time-correlated single-photon-counting (TCSPC) method. The other two lifetimes shortened with increasing excitation intensity. The averaged lifetime of τ_1 and τ_2 is attributed to an effective deactivation time of singlet excitons through singlet–singlet annihilation (SSA). Upon photoexcitaion under ~60 μJ cm^{-2}, the averaged lifetime was estimated to be 11 ps.

In order to extract the formation dynamics of triplet excitons, we subtracted the decay fraction of singlet excitons from the transient absorption decay at 780 nm as shown in Figure 4a. In this

normalization procedure, we assumed no triplet generation at 0 ps because the transient absorption spectrum at 0 ps is in good agreement with that observed under a low excitation intensity as mentioned above. Although there is some uncertainty in the triplet population at 0 ps, the uncertainty is small enough that the triplet formation dynamics can be safely discussed.[41] The triplet formation dynamics can be fitted with the sum of two exponential functions and a constant fraction with the same time constants of τ_1 and τ_2 mentioned above. This agreement in the rise and decay dynamics of singlet and triplet excitons suggests that triplet excitons are rapidly interconverted from singlet excitons with an averaged time constant of 11 ps as will be discussed later. No contribution of τ_3 in the triplet formation dynamics indicates that the triplet formation through the intersystem crossing (ISC) is negligible because of the ISC rate constant as slow as $10^6 - 10^7$ s^{-1} in polyfluorene films.[42,43] The solid line in Figure 4b shows the transient absorption decays of triplet excitons in amorphous PFO films on a time scale of nanoseconds. The transient signals at 780 nm are safely ascribed to triplet excitons because no singlet excitons are survived in this time domain. The decay of the triplet exciton band was fitted with the sum of an exponential function and a constant fraction: $\Delta OD(t) = A \exp(-t/\tau) + B$ with a lifetime of 1.7 ns (A : B = 50 : 50), which was independent of the excitation intensity (see the Supporting Information). The lifetime of 1.7 ns is too short to be assigned to "free" triplet excitons, which decays with a lifetime of ~3.2 μs (see the Supporting Information) as will be discussed later. The triplet absorption signals at 100 ps increased nonlinearly with increasing excitation intensity: the intensity dependence was fitted with a power-law equation of $\Delta OD \propto I^m$ with a slope of $m = 2$ (see the Supporting Information). This finding indicates that a bimolecular reaction such as SSA is involved in the triplet exciton formation as will be discussed later.

-----<<< Figures 3,4 >>>-----

-----<<< Table 1 >>>-----

β-PFO Film: The dynamics of singlet excitons in *β* phase can be observed at 1050 nm selectively. As in the case of the amorphous PFO film, the *β* phase singlet exciton band also decayed faster under higher excitation intensities (in Figure 3, only the decay curve for an excitation intensity of ~60 μJ cm^{-2} is shown by the broken line). The decay curve was fitted with the sum of three exponential functions: $\Delta OD(t) = A_1 \exp(-t/\tau_1) + A_2 \exp(-t/\tau_2) + A_3 \exp(-t/\tau_3)$. The longest lifetime τ_3 was again fixed to a fluorescence lifetime of 390 ps that was evaluated by the TCSPC method. The averaged lifetime of the other two lifetimes was estimated to be 8 ps under ~60 μJ cm^{-2}, suggesting that the SSA proceeds more efficiently in the *β*-PFO film than in the amorphous PFO film.[44]

The formation dynamics of triplet excitons can be deduced by the same procedure as mentioned above. The deduced formation dynamics of triplet excitons was again fitted with the sum of two exponential functions and a constant fraction with the same time constants of τ_1 and τ_2 as fitted to the singlet decay (see the Supporting Information). The coincidence in the rise and decay dynamics of singlet and triplet excitons suggests that triplet excitons are interconverted from singlet excitons as will be discussed later. The broken line in Figure 4b shows the transient absorption decay of triplet excitons in *β*-PFO films on a time scale of nanoseconds. No decay of triplet excitons was observed for the *β*-PFO film in contrast to the distinct decay observed for the amorphous PFO film as will be discussed later.

3. Discussion

3.1. Triplet Exciton Formation. First we discuss the formation mechanism of triplet excitons in the amorphous PFO film. Under an excitation intensity of ~60 μJ cm^{-2}, as mentioned above, triplet excitons are rapidly interconverted from singlet excitons with a time constant of 11 ps. Such a rapid triplet exciton formation would require strong spin mixing between singlet and triplet excitons. Triplet excitons are typically generated through ISC on a time scale of nano- to microseconds, because the ISC is spin-forbidden. Indeed, the ISC rate constant in polyfluorenes has been reported as slow as $10^6 – 10^7$ s^{-1} because of the weak spin–orbit coupling.[42,43] Therefore, ultrafast triplet exciton formation observed

in this study cannot be ascribed to usual ISC. Some reports suggested that the increase in triplet excitons generation yield in solid state than in solution is attributed to the charge recombination into triplet excitons.[39,45] However, this is not the case because hyperfine interaction (HFI) with nuclear magnetic moments, which plays an important role in the interconversion mechanism in organic radicals, is also too weak to explain such a rapid spin flip in picoseconds. A HFI value of ~5 mT reported for PFO[46] corresponds to an interconversion time of several nanoseconds, which is two orders of magnitude slower than the triplet formation time we observed. In other words, polaron pairs still conserve singlet spin state within a few picoseconds, and hence singlet state would be preferentially regenerated by the recombination of polaron pairs in this time domain. Therefore, singlet fission is a most probable scheme to rationalize such a rapid triplet formation. The overall reaction from singlet to triplet exciton in singlet fission is spin-conserving and spin-allowed, and therefore can proceed on a time scale of femto- to picoseconds.[2,3]

We next discuss the energetics for the rapid triplet exciton formation due to singlet fission. For efficient singlet fission, the singlet excited state energy should be higher than twice the triplet excited state energy $E(S) > 2E(T)$. As mentioned before, the energy levels of the lowest singlet and triplet excited states were estimated to be 2.93 and 2.11 eV, respectively. In other words, the singlet fission from the lowest singlet excited state is highly endothermic and hence is thermodynamically unfavorable. Furthermore, the lowest singlet excited state under high excitation intensities is strongly quenched through the SSA. If the annihilation deactivates merely singlet excitons and is not related to the formation of triplet excitons, the formation yield of triplet excitons should be suppressed with increasing excitation intensity. However, triplet excitons are more efficiently formed at higher excitation intensities as mentioned above, suggesting that triplet excitons are efficiently generated from a higher singlet excited state S_n formed by the SSA (singlet fusion). This singlet fusion followed by the singlet fission is thermodynamically favorable because $E(S_n) > 2E(T)$, which has been reported for several materials previously.[27,47–49] We therefore conclude that the rapid triplet exciton formation is attributed to the singlet fusion followed by the singlet fission into triplet excitons as shown in Scheme 1.

3.2. Triplet Exciton Deactivation. For amorphous PFO films, as shown in Figure 4b, about 50% of triplet excitons are deactivated with a lifetime of 1.7 ns. This lifetime is too short to be assigned to "free" triplet excitons because the lifetime of "free" triplet excitons is as long as 3.2 μs. A simple scheme for the singlet fusion followed by the singlet fission is given by Eq. 1[1–3]

$$S_n + S_0 \underset{k_2}{\overset{k_{-2}}{\rightleftarrows}} (TT) \underset{k_1}{\overset{k_{-1}}{\rightleftarrows}} T_1 + T_1 \qquad (1)$$

where (TT) is an intermediate pair state (triplet pair state). In this state, triplet excitons are assumed to be close enough to collide with each other whose spin functions are coupled into a pure singlet state. The reverse reaction of singlet fission is equivalent to the TTA, and thus is also spin-allowed for the same reason. Therefore, this rapid decay is attributed to the back reaction of triplet excitons into two singlet states through the TTA.[1,12,27,43,50–52] The deactivation time of triplet excitons was independent of the excitation intensity (Supporting Information), suggesting that two triplet excitons generated by singlet fission are still close to each other in this time domain and hence can be considered as a pair state. In other words, 50% of the triplet pair states deactivates geminately through the intensity-independent TTA. The rest of triplet excitons (~50%) remain constantly. The constant component is ascribed to dissociated free triplet excitons, which would survive for even as long as microseconds. Here we assumed that spectroscopic properties of the triplet pair state such as the transient absorption spectra and the molar absorption coefficient are identical to those of free triplet excitons because the interaction between a pair of two triplet excitons is considered to be very weak.[1–3] In contrast, no triplet decay is observed for *β*-PFO films, suggesting that all the triplet pairs are dissociated into free triplet excitons. Such morphology dependence of the triplet formation in PFO films will be discussed below in details.

3.3. Morphology Dependence of Singlet Fission Efficiency. First, we discuss singlet fusion followed by the triplet pair formation: $S_1 + S_1 \rightarrow S_n + S_0 \rightarrow (TT)$. As shown in Figure 3, the higher singlet excited state S_n is formed more efficiently in the *β*-PFO than in the amorphous PFO film. On the

other hand, as shown in Figure 4b, the triplet pair formation is about two times more efficient in the amorphous PFO than in the *β*-PFO film, indicating that the singlet fission from the S_n state is more efficient in the amorphous PFO rather than in the ordered *β*-PFO film, which is in sharp contrast to the singlet fission in small molecules: singlet fission is typically more efficient in molecular crystals than in less ordered films.[28,29] The decrease in the fission efficiency in the *β*-PFO film is attributable to the presence of another relaxation pathway from the S_n state. As shown in Figure 2b, polarons are additionally generated in the *β*-PFO film. Assuming that the molar absorption coefficients of triplet exciton and polaron are in the same order of $5 - 6 \times 10^4$ M^{-1} cm^{-1} as reported previously,[39,53] the formation rate of triplet pairs is estimated to be almost the same as that of polarons in the *β*-PFO film. This is in good agreement with about two times lower triplet pair formation yield in the *β*-PFO film than in the amorphous PFO film. Therefore, the decrease in the triplet pair formation efficiency in ordered *β*-PFO films is attributed to the comparably efficient polaron formation (Scheme 1). This finding is consistent with our previous study on triplet formation in amorphous RRa-P3HT and crystalline RR-P3HT films: triplet excitons are efficiently generated through singlet fission in RRa-P3HT while no triplet excitons are generated in RR-P3HT films but instead polaron pairs are preferentially generated.[27] The efficient charge generation in *β*-PFO and RR-P3HT is probably attributed to the larger interchain interaction in ordered phases.

We next move onto the triplet pair dissociation into two free triplet excitons, $(TT) \rightarrow T_1 + T_1$. As shown in Figure 4b, about a half of triplet pairs are deactivated in the amorphous PFO film through the TTA with a time constant of 1.7 ns, while no triplet pair decay is observed in the *β*-PFO film. In other words, the triplet pair dissociation is more efficient in the *β*-PFO than in the amorphous PFO film, although the triplet pair formation is two times more efficient in the amorphous PFO than in the *β*-PFO film as mentioned above. As a result, the overall triplet generation yield is comparable in these films. In the triplet pair dissociation, the triplet exciton diffusion plays a key role as reported previously.[50–52] In an extreme case, the triplet excitons are easily deactivated through the TTA in a covalently linked tetracene dimer although the efficient triplet dissociation is observed in tetracene single crystals.[51,52]

Owing to the planner conformation in the β-PFO film, the triplet exciton diffusion coefficient would be larger in the β-PFO film than in amorphous PFO films because of the larger intrachain and interchain electronic couplings in the β-PFO film, which is beneficial for the Dexter energy transfer.[1,43,54] We therefore conclude that the efficient triplet pair dissociation in β-PFO is due to the larger triplet exciton diffusion coefficient. In summary, the triplet pair formation efficiency is more efficient in amorphous PFO than in ordered β-PFO films because of a competitive relaxation pathway of the efficient charge generation in β-PFO film. On the other hand, the triplet pair dissociation is more efficient in β-PFO than in amorphous PFO films because of larger triplet exciton diffusion coefficient in ordered phases. As a result, the overall triplet generation yield is comparable in amorphous and β-PFO films.

3.4. Material Design for Efficient Singlet Fission in Conjugated Polymers. Most of the singlet fission mechanisms reported for conjugated polymers is the singlet fission not from the lowest singlet excited state but from a hot singlet excited state.[20–27] This is in contrast to the singlet fission in molecular crystals such as tetracene and pentacene,[2,3,12–19] which occurs from the lowest singlet excited state efficiently. This is probably due to the small energy gap between the lowest singlet excited state (S_1 state) and the lowest triplet excited state (T_1 state) ΔE_{ST} in conjugated polymers with delocalized π system more than in small molecules. In such a case, the energy level of the S_1 state is lower than twice that of the T_1 state: the singlet fission from the S_1 state is thermodynamically unfavorable and hence inefficient. As described above, the singlet fission from a higher singlet excited state is in competition with polaron generation. This is probably because higher singlet excited states generally are more mixed with charge transfer states. Indeed, efficient polaron formations from higher singlet excited states have been reported for many conjugated polymers.[1,27,30,38,39,55–57] We therefore propose that the singlet fission from the S_2 state would be an alternative for conjugated polymers. For example, some low-bandgap polymers have the S_1 band at around 800 nm (1.55 eV) and the S_2 band at around 400 nm (3.1 eV). The T_1 state is roughly estimated to be ~1 eV assuming that ΔE_{ST} is 0.5 eV. Thus, the singlet fission from the S_2 state is thermodynamically possible ($E(S_2) \geq 2E(T_1)$). Considering the high triplet

exciton diffusion required for efficient dissociation into two triplets, low-bandgap crystalline polymers would be suitable for efficient singlet fission in conjugated polymers.

4. Conclusions

We have studied the singlet fission dynamics in PFO films by transient absorption spectroscopy. Under an excitation intensity of ~60 μJ cm^{-2}, triplet excitons are rapidly interconverted from singlet excitons with a time constant of 11 ps in amorphous PFO and 8 ps in *β*-PFO films, which is too fast to be assigned to ISC from singlet to triplet excitons or the recombination from singlet polaron pairs to triplet excitons. Therefore, singlet fission is a most probable scheme to rationalize such a rapid triplet exciton formation. From the excitation intensity dependence of the triplet exciton formation efficiency, we conclude that the rapid triplet exciton formation in PFO films is attributed to singlet fission from a higher singlet excited state S_n formed by the SSA (singlet fusion). The triplet pair formation efficiency is about two times more efficient in amorphous PFO than in ordered *β*-PFO films because of a competitive relaxation pathway of the efficient charge generation in *β*-PFO films. On the other hand, the triplet pair dissociation is more efficient in *β*-PFO than in amorphous PFO films because of larger triplet exciton diffusion coefficient in ordered phase. As a result, the overall triplet generation yield is comparable in these films. For efficient singlet fission in conjugated polymers, we propose that low-bandgap crystalline polymers would be suitable for efficient singlet fission in conjugated polymers.

5. Experimental Section

Sample Preparation. PFO was purchased from American Dye Source, Inc. and used without further purification. Amorphous PFO films were prepared by spincoating from chloroform solution and *β*-PFO films were prepared by spincoating from chloroform solution with an additive of 1,8-diiodooctane (DIO) (2% by volume). For transient absorption measurements, a sapphire substrate was used to prevent waveguiding and amplified spontaneous emission,[58,59] while the other experiments have done with a quartz substrate. The film thickness was about 100 nm.

Measurements. UV–visible absorption and photoluminescence spectra of PFO films were measured with a UV–visible spectrophotometer (Hitachi, U-3500) and a fluorescence spectrophotometer (Hitachi, F-4500) equipped with a red-sensitive photomultiplier (Hamamatsu, R928F), respectively. Phosphorescence spectra were collected in a time domain longer than 2 ms after the excitation by using a mechanical chopper incorporated in the fluorescence spectrophotometer (Hitachi, F-4500). Photoluminescence decay was measured by the time-correlated single-photon-counting (TCSPC) method (Horiba Jobin Yvon, FluoroCube). The excitation wavelength was 375 nm. The total instrument response function is an FWHM of ca. 280 ps. A weak excitation power (~nJ cm^{-2}) was used in the measurement to prevent singlet–singlet annihilation.

Transient absorption data were collected with a pump and probe femtosecond transient spectroscopy system. This system consists of a transient absorption spectrometer (Ultrafast Systems, Helios) and a regenerative amplified Ti:sapphire laser (Spectra-Physics, Hurricane). The amplified Ti:sapphire laser provided 800 nm fundamental pulses at a repetition rate of 1 kHz with an energy of 0.9 mJ and a pulse width of 100 fs (FWHM), which were split into two optical beams with a beam splitter to generate pump and probe pulses. One fundamental beam was converted into pump pulses at 400 nm with a second harmonic generator (Spectra-Physics, TP-F). The other fundamental beam was converted into white light pulses employed as probe pulses in the wavelength region from 400 to 1700 nm. The pump pulses were modulated mechanically with a repetition rate of 500 Hz. The temporal evolution of the probe intensity was recorded with a CMOS linear sensor (Ultrafast Systems, SPEC-VIS) for the visible measurement and with an InGaAs linear diode array sensor (Ultrafast Systems, SPEC-NIR) for the near-IR measurement. The transient absorption spectra and decays were collected over the time range from −5 ps to 6 ns. Typically, 1500 laser shots were averaged at each delay time to obtain a detectable absorbance change as small as ~10^{-4}. In order to cancel out the orientation effects on the dynamics, the polarization direction of the linearly polarized probe pulse was set at a magic angle of 54.7 ° with respect to that of the pump pulse. The sample films were sealed in a quartz cuvette purged with N_2. Note that the transient absorption spectra and dynamics were highly reproducible even after the several

times measurements. In other words, the laser irradiation had negligible effects on the sample degradation at least under this experimental condition.

Acknowledgments. This work was partly supported by JST PRESTO program (Photoenergy and Conversion Systems and Materials for the Next-Generation Solar Cells), the Global COE program (International Center for Integrated Research and Advanced Education in Materials Science) from the Ministry of Education, Culture, Sports, Science, and Technology, Japan. Y. Tamai also thanks Research Fellowships of the Japan Society for the Promotion of Science for Young Scientists.

Supporting Information Available: Singlet energy transfer dynamics in *β*-PFO films, monomolecular triplet excitons lifetime, excitation intensity dependence of the triplet exciton generation and decay, and triplet exciton formation dynamics in *β*-PFO film. This material is available free of charge via the Internet at http://pubs.acs.org.

References and Notes

(1) Pope, M.; Swenberg, C. E. *Electronic Processes in Organic Crystals and Polymers*; Oxford University Press: Oxford, U.K., 1999.

(2) Smith, M. B.; Michl, J. Singlet Fission. *Chem. Rev.* **2010**, *110*, 6891–6936.

(3) Smith, M. B.; Michl, J. Recent Advances in Singlet Fission. *Annu. Rev. Phys. Chem.* **2013**, *64*, 361–386.

(4) Hanna, M. C.; Nozik, A. J. Solar Conversion Efficiency of Photovoltaic and Photoelectrolysis Cells with Carrier Multiplication Absorbers. *J. Appl. Phys.* **2006**, *100*, 074510.

(5) Rao, A.; Wilson, M. W. B.; Hodgkiss, J. M.; Albert-Seifried, S.; Bässler, H.; Friend, R. H. Exciton Fission and Charge Generation via Triplet Excitons in Pentacene/C_{60} Bilayers. *J. Am. Chem. Soc.* **2010**, *132*, 12698–12703.

(6) Jadhav, P. J.; Mohanty, A.; Sussman, J.; Lee, J.; Baldo, M. A. Singlet Exciton Fission in Nanostructured Organic Solar Cells. *Nano Lett.* **2011**, *11*, 1495–1498.

(7) Ehrler, B.; Wilson, M. W. B.; Rao, A.; Friend, R. H.; Greenham, N. C. Singlet Exciton Fission-Sensitized Infrared Quantum Dot Solar Cells. *Nano Lett.* **2012**, *12*, 1053–1057.

(8) Ehrler, B.; Walker, B. J.; Böhm, M. L.; Wilson, M. W. B.; Vaynzof, Y.; Friend, R. H.; Greenham, N. C. In Situ Measurement of Exciton Energy in Hybrid Singlet-Fission Solar Cells. *Nat. Commun.* **2012**, *3*, 1019.

(9) Chan, W.-L.; Tritsch, J. R.; Zhu, X.-Y. Harvesting Singlet Fission for Solar Energy Conversion: One- versus Two-Electron Transfer from the Quantum Mechanical Superposition. *J. Am. Chem. Soc.* **2012**, *134*, 18295–18302.

(10) Ehrler, B.; Musselman, K. P.; Böhm, M. L.; Friend, R. H.; Greenham, N. C. Hybrid Pentacene/a-Silicon Solar Cells Utilizing Multiple Carrier Generation via Singlet Exciton Fission. *Appl. Phys. Lett.* **2012**, *101*, 153507.

(11) Singh, S.; Jones, W. J.; Siebrand, W.; Stoicheff, B. P.; Schneider, W. G. Laser Generation of Excitons and Fluorescence in Anthracene Crystals. *J. Chem. Phys.* **1965**, *42*, 330–342.

(12) Thorsmølle, V. K.; Averitt, R. D.; Demsar, J.; Smith, D. L.; Tretiak, S.; Martin, R. L.; Chi, X.; Crone, B. K.; Ramirez, A. P.; Taylor, A. J. Morphology Effectively Controls Singlet-Triplet Exciton Relaxation and Charge Transport in Organic Semiconductors. *Phys. Rev. Lett.* **2009**, *102*, 017401.

(13) Johnson, J. C.; Nozik, A. J.; Michl, J. High Triplet Yield from Singlet Fission in a Thin Film of 1,3-Diphenylisobenzofuran. *J. Am. Chem. Soc.* **2010**, *132*, 16302–16303.

(14) Burdett, J. J.; Müller, A. M.; Gosztola, D.; Bardeen, C. J. Excited State Dynamics in Solid and Monomeric Tetracene: The Roles of Superradiance and Exciton Fission. *J. Chem. Phys.* **2010**, *133*, 144506.

(15) Rao, A.; Wilson, M. W. B.; Albert-Seifried, S.; Di Pietro, R.; Friend, R. H. Photophysics of Pentacene Thin Films: The Role of Exciton Fission and Heating Effects. *Phys. Rev. B* **2011**, *84*, 195411.

(16) Burdett, J. J.; Gosztola, D.; Bardeen, C. J. The Dependence of Singlet Exciton Relaxation on Excitation Density and Temperature in Polycrystalline Tetracene Thin Films: Kinetic Evidence for a Dark Intermediate State and Implications for Singlet Fission. *J. Chem. Phys.* **2011**, *135*, 214508.

(17) Wilson, M. W. B.; Rao, A.; Clark, J.; Kumar, R. S. S.; Brida, D.; Cerullo, G.; Friend, R. H. Ultrafast Dynamics of Exciton Fission in Polycrystalline Pentacene. *J. Am. Chem. Soc.* **2011**, *133*, 11830–11833.

(18) Zimmerman, P. M.; Bell, F.; Casanova, D.; Head-Gordon, M. Mechanism for Singlet Fission in Pentacene and Tetracene: From Single Exciton to Two Triplets. *J. Am. Chem. Soc.* **2011**, *133*, 19944–19952.

(19) Ma, L.; Zhang, K.; Kloc, C.; Sun, H.; Michel-Beyerle, M. E.; Gurzadyan, G. G. Singlet Fission in Rubrene Single Crystal: Direct Observation by Femtosecond Pump–Probe Spectroscopy. *Phys. Chem. Chem. Phys.* **2012**, *14*, 8307–8312.

(20) Austin, R. H.; Baker, G. L.; Etemad, S.; Thompson, R. Magnetic Field Effects on Triplet Exciton Fission and Fusion in a Polydiacetylene. *J. Chem. Phys.* **1989**, *90*, 6642–6646.

(21) Kraabel, B.; Hulin, D.; Aslangul, C.; Lapersonne-Meyer, C.; Schott, M. Triplet Exciton Generation, Transport and Relaxation in Isolated Polydiacetylene Chains: Subpicosecond Pump-Probe Experiments. *Chem. Phys.* **1998**, *227*, 83–98.

(22) Lanzani, G.; Stagira, S.; Cerullo, G.; De Silvestri, S.; Comoretto, D.; Moggio, I.; Cuniberti, C.; Musso, G. F.; Dellepiane, G. Triplet Exciton Generation and Decay in a Red Polydiacetylene Studied by Femtosecond Spectroscopy. *Chem. Phys. Lett.* **1999**, *313*, 525–532.

(23) Lanzani, G.; Cerullo, G.; Zavelani-Rossi, M.; De Silvestri, S. Triplet-Exciton Generation Mechanism in a New Soluble (Red-Phase) Polydiacetylene. *Phys. Rev. Lett.* **2001**, *87*, 187402.

(24) Wohlgenannt, M.; Graupner, W.; Österbacka, R.; Leising, G.; Comoretto, D.; Vardeny, Z. V. Singlet Fission in Luminescent and Nonluminescent π–conjugated Polymers. *Synth. Met.* **1999**, *101*, 267–268.

(25) Wohlgenannt, M.; Graupner, W.; Leising, G.; Vardeny, Z. V. Photogeneration and Recombination Processes of Neutral and Charged Excitations in Films of a Ladder-type Poly(*para*-phenylene). *Phys. Rev. B* **1999**, *60*, 5321–5330.

(26) Österbacka, R.; Wohlgenannt, M.; Shkunov, M.; Chinn, D.; Vardeny, Z. V. Excitons, Polarons, and Laser Action in Poly(*p*-phenylene vinylene) Films. *J. Chem. Phys.* **2003**, *118*, 8905–8916.

(27) Guo, J.; Ohkita, H.; Benten, H.; Ito, S. Near-IR Femtosecond Transient Absorption Spectroscopy of Ultrafast Polaron and Triplet Exciton Formation in Polythiophene Films with Different Regioregularities. *J. Am. Chem. Soc.* **2009**, *131*, 16869–16880.

(28) Marciniak, H.; Fiebig, M.; Huth, M.; Schiefer, S.; Nickel, B.; Selmaier, F.; Lochbrunner, S. Ultrafast Exciton Relaxation in Microcrystalline Pentacene Films. *Phys. Rev. Lett.* **2007**, *99*, 176402.

(29) Marciniak, H.; Pugliesi, I.; Nickel, B.; Lochbrunner, S. Ultrafast Singlet and Triplet Dynamics in Microcrystalline Pentacene Films. *Phys. Rev. B* **2009**, *79*, 235318.

(30) Gulbinas, V.; Zaushitsyn, Y.; Bässler, H.; Yartsev, A.; Sundström, V. Dynamics of Charge Pair Generation in Ladder-type Poly(para-phenylene) at Different Excitation Photon Energies. *Phys. Rev. B* **2004**, *70*, 035215.

(31) Knaapila, M.; Winokur, M. J. Structure and Morphology of Polyfluorenes in Solutions and the Solid State. *Adv. Polym. Sci.* **2008**, *212*, 227–272.

(32) Peet, J.; Brocker, E.; Xu, Y.; Bazan, G. C. Controlled *β*-Phase Formation in Poly(9,9-di-*n*-octylfluorene) by Processing with Alkyl Additives. *Adv. Mater.* **2008**, *20*, 1882–1885.

(33) Grell, M.; Bradley, D. D. C.; Ungar, G.; Hill, J.; Whitehead, K. S. Interplay of Physical Structure and Photophysics for a Liquid Crystalline Polyfluorene. *Macromolecules* **1999**, *32*, 5810–5817.

(34) Chen, S. H.; Su, A. C.; Chen, S. A. Noncrystalline Phases in Poly(9,9-di-*n*-octyl-2,7-fluorene). *J. Phys. Chem. B* **2005**, *109*, 10067–10072.

(35) Monkman, A.; Rothe, C.; King, S.; Dias, F. Polyfluorene Photophysics. *Adv. Polym. Sci.* **2008**, *212*, 187–225.

(36) Ariu, M.; Sims, M.; Rahn, M. D.; Hill, J.; Fox, A. M.; Lidzey, D. G.; Oda, M.; Cabanillas-Gonzalez, J.; Bradley, D. D. C. Exciton Migration in *β*-Phase Poly(9,9-dioctylfluorene). *Phys. Rev. B* **2003**, *67*, 195333.

(37) Khan, A. L. T.; Sreearunothai, P.; Herz, L. M.; Banach, M. J.; Köhler, A. Morphology-Dependent Energy Transfer within Polyfluorene Thin Films. *Phys. Rev. B* **2004**, *69*, 085201.

(38) Stevens, M. A.; Silva, C.; Russell, D. M.; Friend, R. H. Exciton Dissociation Mechanisms in the Polymeric Semiconductors Poly(9,9-dioctylfluorene) and Poly(9,9-dioctylfluorene-co-benzothiadiazole). *Phys. Rev. B* **2001**, *63*, 165213.

(39) Cadby, A. J.; Lane, P. A.; Mellor, H.; Martin, S. J.; Grell, M.; Giebeler, C.; Bradley, D. D. C.; Wohlgenannt, M.; An, C.; Vardeny, Z. V. Film Morphology and Photophysics of Polyfluorene. *Phys. Rev. B* **2000**, *62*, 15604–15609.

(40) Hayer, A.; Khan, A. L. T.; Friend, R. H.; Köhler, A. Morphology Dependence of the Triplet Excited State Formation and Absorption in Polyfluorene. *Phys. Rev. B* **2005**, *71*, 241302.

(41) The transient absorption spectrum at 0 ps can be well reproduced with only the singlet exciton absorption spectrum, indicating that triplet population at 0 ps is negligibly small. On the basis of spectral simulation, the uncertainty of the triplet population at 0 ps is estimated to be 1 mOD at most, which corresponds to about 15% of the total generated triplet excitons. Such small uncertainty of the triplet population (about 15% at most) does not affect the triplet build up time at all. Thus, the following analysis on the triplet formation dynamics is independent of this normalization procedure.

(42) King, S.; Rothe, C.; Monkman, A. Triplet Build in and Decay of Isolated Polyspirobifluorene Chains in Dilute Solution. *J. Chem. Phys.* **2004**, *121*, 10803–10808.

(43) Köhler, A.; Bässler, H. Triplet States in Organic Semiconductors. *Mater. Sci. Eng. R* **2009**, *66*, 71–109.

(44) Shaw, P. E.; Ruseckas, A.; Peet, J.; Bazan, G. C.; Samuel, I. D. W. Exciton–Exciton Annihilation in Mixed-Phase Polyfluorene Films. *Adv. Funct. Mater.* **2010**, *20*, 155–161.

(45) King, S. M.; Rothe, C.; Dai, D.; Monkman, A. P. Femtosecond Ground State Recovery: Measuring the Intersystem Crossing Yield of Polyspirobifluorene. *J. Chem. Phys.* **2006**, *124*, 234903.

(46) Sheng, Y.; Nguyen, T. D.; Veeraraghavan, G.; Mermer, Ö.; Wohlgenannt, M.; Qiu, S.; Scherf, U. Hyperfine Interaction and Magnetoresistance in Organic Semiconductors. *Phys. Rev. B* **2006**, *74*, 045213.

(47) Katoh, R.; Kotani, M. Fission of a Higher Excited State Generated by Singlet Exciton Fusion in an Anthracene Crystal. *Chem. Phys. Lett.* **1992**, *196*, 108–112.

(48) Katoh, R.; Kotani, M.; Hirata, Y.; Okada, T. Triplet Exciton Formation in a Benzophenone Single Crystal Studied by Picosecond Time-Resolved Absorption Spectroscopy. *Chem. Phys. Lett.* **1997**, *264*, 631–635.

(49) Watanabe, S.; Furube, A.; Katoh, R. Generation and Decay Dynamics of Triplet Excitations in Alq3 Thin Films under High-Density Excitation Conditions. *J. Phys. Chem. A* **2006**, *110*, 10173–10178.

(50) Arnold, S.; Alfano, R. R.; Pope, M.; Yu, W.; Ho, P.; Selsby, R.; Tharrats, J.; Swenberg, C. E. Triplet Exciton Caging in Two Dimensions. *J. Chem. Phys.* **1976**, *64*, 5104–5114.

(51) Müller, A. M.; Avlasevich, Y. S.; Müllen, K.; Bardeen, C. J. Evidence for Exciton Fission and Fusion in a Covalently Linked Tetracene Dimer. *Chem. Phys. Lett.* **2006**, *421*, 518–522.

(52) Müller, A. M.; Avlasevich, Y. S.; Schoeller, W. W.; Müllen, K.; Bardeen, C. J. Exciton Fission and Fusion in Bis(tetracene) Molecules with Different Covalent Linker Structures. *J. Am. Chem. Soc.* **2007**, *129*, 14240–14250.

(53) Takeda, N.; Asaoka, S.; Miller, J. R. Nature and Energies of Electrons and Holes in a Conjugated Polymer, Polyfluorene. *J. Am. Chem. Soc.* **2006**, *128*, 16073–16082.

(54) Turro, N. J. *Modern Molecular Photochemistry*; University Science Books: Sausalito, CA, 1978.

(55) Silva, C.; Dhoot, A. S.; Russell, D. M.; Stevens, M. A.; Arias, A. C.; MacKenzie, J. D.; Greenham, N. C.; Friend, R. H. Efficient Exciton Dissociation via Two-Step Photoexcitation in Polymeric Semiconductors. *Phys. Rev. B* **2001**, *64*, 125211.

(56) Dicker, G.; de Haas, M. P.; Siebbeles, L. D. A.; Warman, J. M. Electrodeless Time-Resolved Microwave Conductivity Study of Charge-Carrier Photogeneration in Regioregular Poly(3-hexylthiophene) Thin Films. *Phys. Rev. B* **2004**, *70*, 045203.

(57) Scholes, G. D. Insights into Excitons Confined to Nanoscale Systems: Electron–Hole Interaction, Binding Energy, and Photodissociation. *ACS Nano* **2008**, *2*, 523–537.

(58) Nisoli, M.; Stagira, S.; Zavelani-Rossi, M.; De Silvestri, S.; Mataloni, P.; Zenz, C. Ultrafast Light-Emission Processes in Poly(*para*-phenylene)-type Ladder Polymer Films. *Phys. Rev. B* **1999**, *59*, 11328–11332.

(59) Azuma, H.; Kobayashi, T.; Shim, Y.; Mamedov, N.; Naito, H. Amplified Spontaneous Emission in α-Phase and β-Phase Polyfluorene Waveguides. *Org. Electron.* **2007**, *8*, 184–188.

FIGURE CAPTIONS

Figure 1. (a) Absorption, (b) fluorescence, and (c) phosphorescence spectra of amorphous PFO (broken) and *β*-PFO (solid) films. The photoluminescence spectra were measured with the 360 nm excitation. The phosphorescence spectra were measured at 77 K by using a mechanical chopper. The inset in panel (a) shows the chemical structure of PFO.

Figure 2. Transient absorption spectra of (a) amorphous PFO and (b) *β*-PFO films excited at 400 nm (~60 μJ cm^{-2}) measured at 0, 1, 10, 100, 1000, and 3000 ps after the laser excitation from top to bottom. The insets show the normalized transient absorption spectra measured at 0 and 3000 ps.

Figure 3. Transient absorption decays of PFO films measured at 1050 nm (solid lines: amorphous PFO films and broken line: *β*-PFO films). The excitation intensity was varied over 7, 14, 20, 40, 60 and 60 μJ cm^{-2} from top to bottom. The gray lines represent the fitting curves with the sum of three exponential functions: $\Delta OD(t) = A_1 \exp(-t/\tau_1) + A_2 \exp(-t/\tau_2) + A_3 \exp(-t/\tau_3)$ where τ_3 is fixed to a fluorescence lifetime of 410 ps (solid lines) and 390 ps (broken line) evaluated by the TCSPC method.

Figure 4. (a) Normalized transient absorption decays of amorphous PFO films excited at 400 nm (~60 μJ cm^{-2}) measured at 780 nm (circles) and 1050 nm (singlet exciton, triangles). The transient signals at 780 and 1050 nm were normalized at 0 ps. The square symbols are obtained by subtracting the normalized transient absorption signal at 1050 nm from that at 780 nm, which represent the time evolution of triplet excitons. The solid line represents the fitting curve with the sum of two exponential functions and a constant fraction with the same time constants of τ_1 and τ_2 in Figure 3. The inset shows the initial part of the decays on a shorter time scale of 0 – 25 ps in semi-logarithmic scale. (b) Transient absorption decays of amorphous (solid line, measured at 780 nm) and *β*-PFO (broken line, measured at 850 nm) films on a time scale of nanoseconds under a fluence of 60 μJ cm^{-2}.

SCHEME TITLES

Scheme 1. Energy Diagrams for Singlet Fission in PFO Films.

TABLES

Table 1. Fitting Parameters for Transient Absorption Decays of PFO Films.

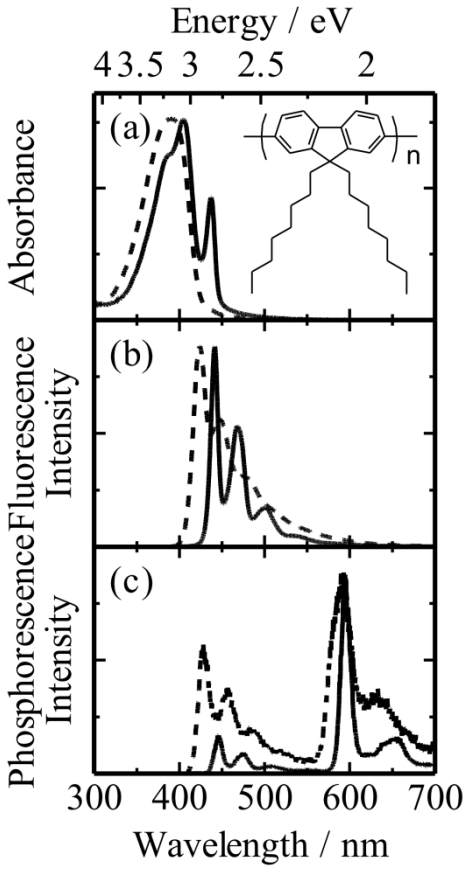
Energy / eV
4
3.5
3
2.5
2
(a)
n
Absorbance
(b)
Fluorescence Intensity
(c)
Phosphorescence Intensity
300
400
500
600
700
Wavelength / nm

Figure 1

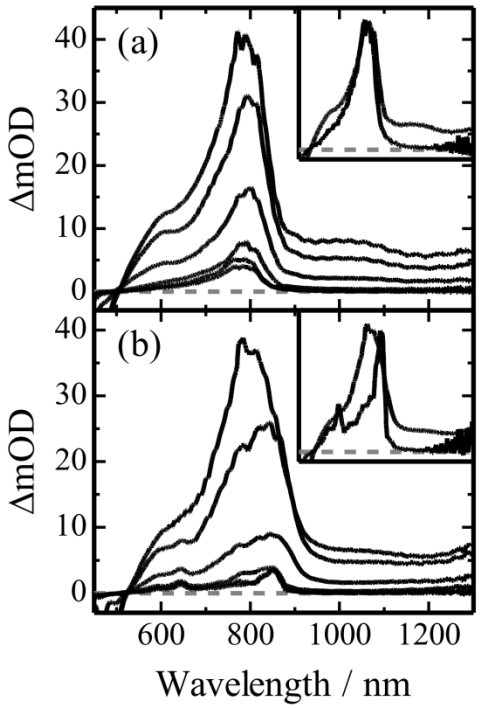

Figure 2

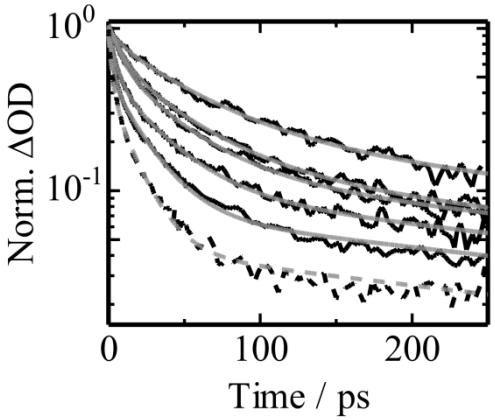

Figure 3

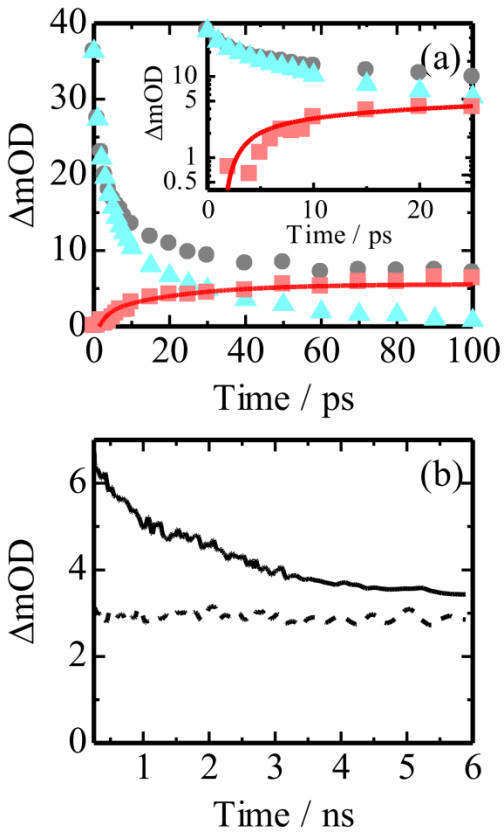

Figure 4

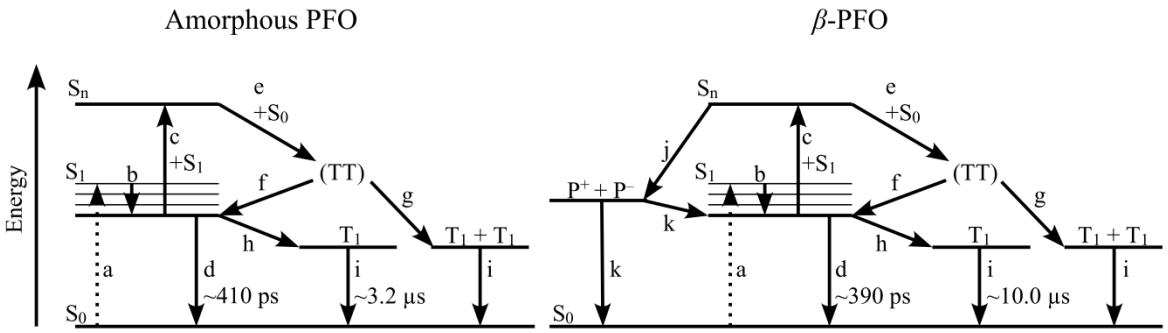

Key: (a) photon absorption, (b) vibrational relaxation, (c) singlet–singlet annihilation (SSA, singlet fusion), (d) radiative and non-radiative deactivations, (e) singlet fission, (f) back recombination of triplet pairs through triplet–triplet annihilation (TTA, triplet fusion), (g) triplet pair dissociation, (h) intersystem crossing (k_{ISC}), (i) monomolecular triplet deactivation, (j) polaron formation, (k) polaron recombination.

Scheme 1

Table 1

Sample	Intensity / μJ cm^{-2}	$A_{1,2\text{-ave}}$ / %	$\tau_{1,2\text{-ave}}$ / ps	A_3 / %	τ_3 / ps
Amorphous PFO	7	77	43	23	410
	14	86	29	14	410
	20	87	24	13	410
	40	90	17	10	410
	60	93	11	7	410
β-PFO	60	95	8	5	390

Transient absorption decays at 1050 nm were fitted with the sum of three exponential functions: $\Delta OD(t) = A_1 \exp(-t/\tau_1) + A_2 \exp(-t/\tau_2) + A_3 \exp(-t/\tau_3)$. The longest lifetime τ_3 was fixed to a fluorescence lifetime of 410 ps for amorphous PFO and 390 ps for β-PFO films evaluated by the TCSPC method for all excitation intensities. The fraction $A_{1,2\text{-ave}}$ and the lifetime $\tau_{1,2\text{-ave}}$ represent the total fraction of A_1 and A_2, and the averaged lifetime of τ_1 and τ_2, respectively.

Table of Contents graphic